

**Hyperspectral analysis at Angularli uranium deposit, Northern Territory.
BR Smith and P Sinclair, 2025.
Northern Territory Geological Survey, Record 2025-006.**

Appendix 3

Analysis of sample CP17BRS014. NVCL project FY18 – Technical Note.
M LeGras, M Verrall M and C Laukamp, CSIRO Mineral Resources

NTGS Technical Note 2017-008

THIS PAGE LEFT INTENTIONALLY BLANK

Analysis of sample CP17BRS014

NVCL project FY18 – Technical Note

LeGras, M., Verrall, M., Laukamp, C.

CSIRO Mineral Resources, 26 Dick Perry Avenue, Kensington, 6151 WA

Introduction

HyLogging of drillcore by the Northern Territory Geological Survey revealed an unusual spectral response in the VNIR and SWIR for sample CP17BRS014 (Figure 1). Investigation of the SWIR and TIR spectra of this samples suggested presence of predominantly white mica and quartz. Some of the observed absorption features may indicate the presence of rare-earth elements. The sample was further characterised by SEM (Philips XL40) and XRF (Bruker M4 Tornado) at the Australian Resources Research Centre to evaluate the presence of REEs, and determine which mineralogical phase they are contained within.

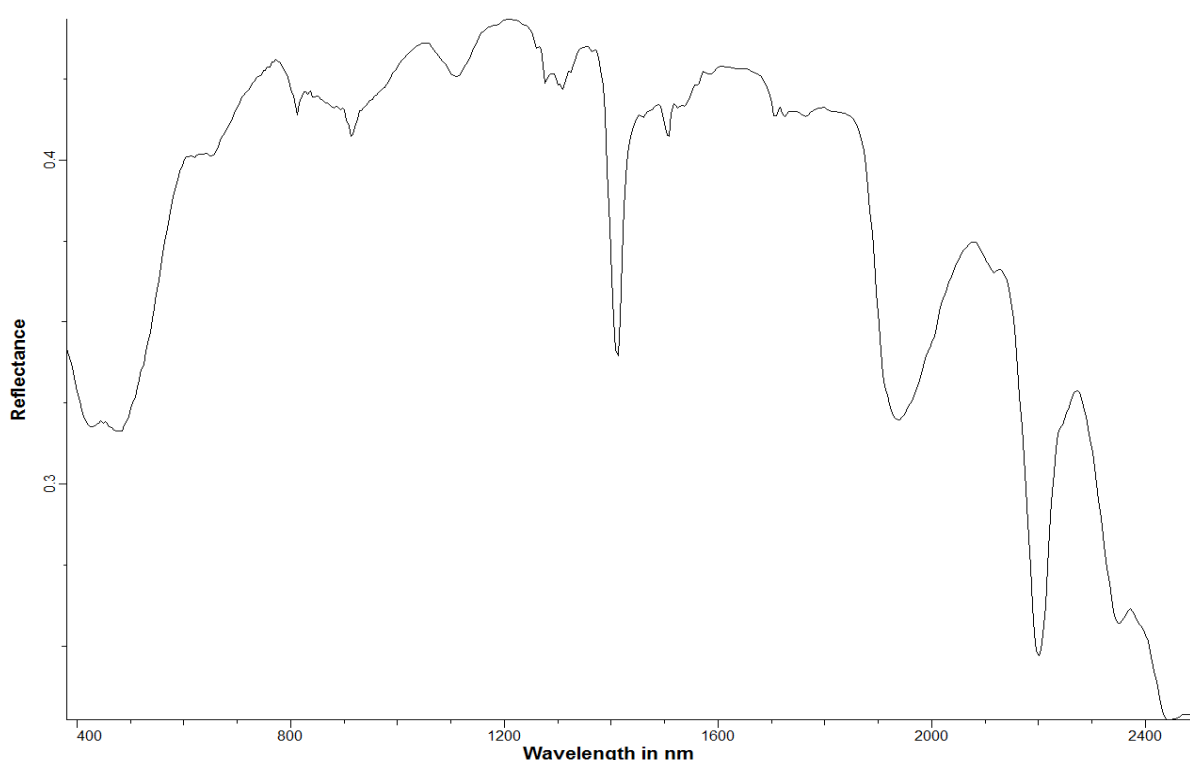


Figure 1 HyLogger spectra of CP17BRS014 showing unusual features in the VNIR to SWIR region (courtesy of Belinda Smith, NTGS).

XRF

XRF mapping illustrates chemical variation and mineralogical relationships across the sample. Two zones are apparent in sample CP17BRS014 and can be defined by the presence of xenotime. Rutile and apatite are much less likely to occur in areas where xenotime is abundant (Figure 2).

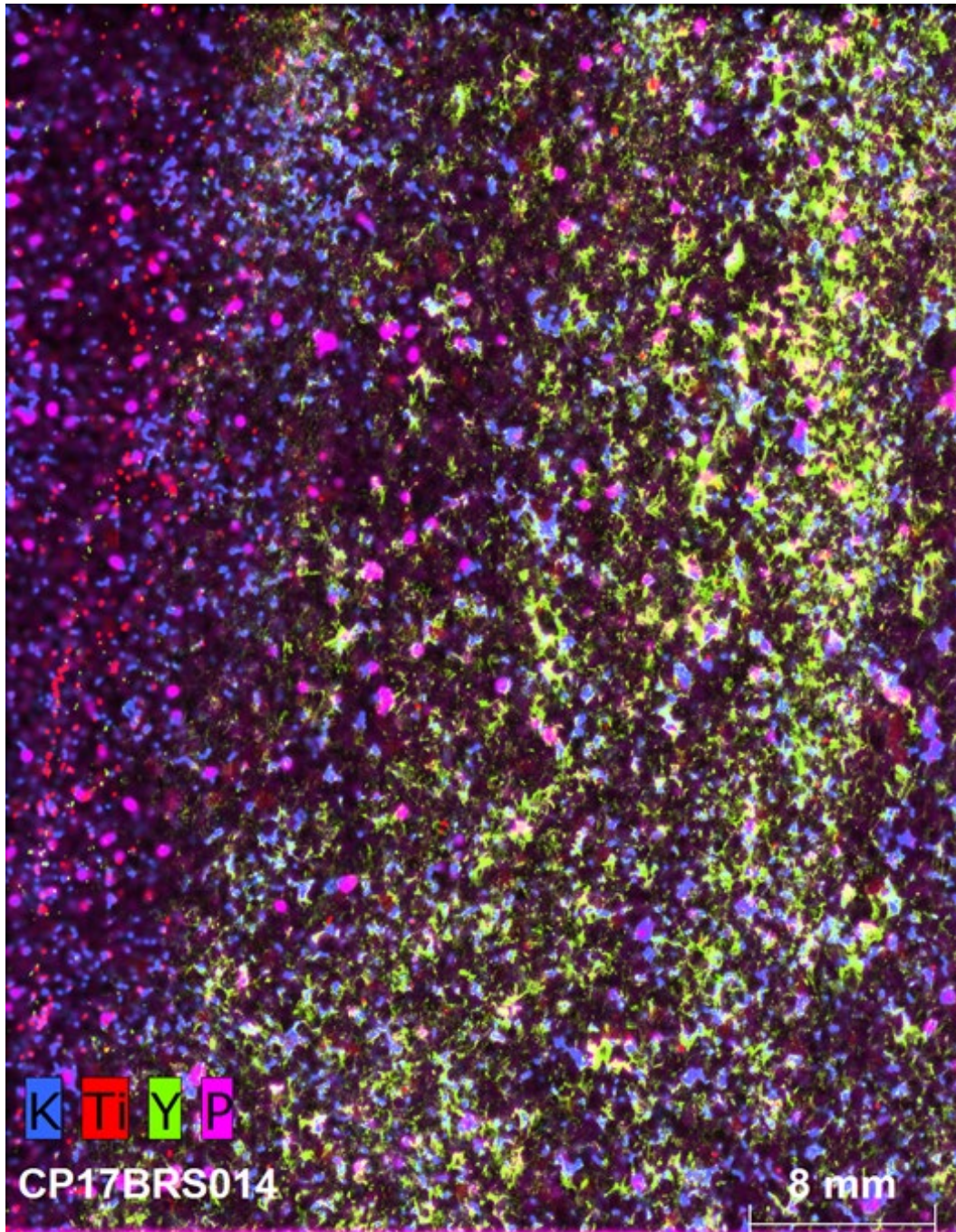


Figure 2 XRF map of CP17BRS014. Effectively, K maps muscovite; Ti rutile; Y xenotime and P apatite.

SEM

SEM analysis of the sample found it to consist mostly of quartz, with muscovite, xenotime, apatite and rutile (Figures 3, 4 and 5). The xenotime (Figure 3) was found to contain several REEs (Figure 6). No REEs were detected in any other phases.

SEM-EDS analyses of the sheet silicate mineral (Figure 7) indicate that this phase is closer to a muscovitic than an illitic composition.

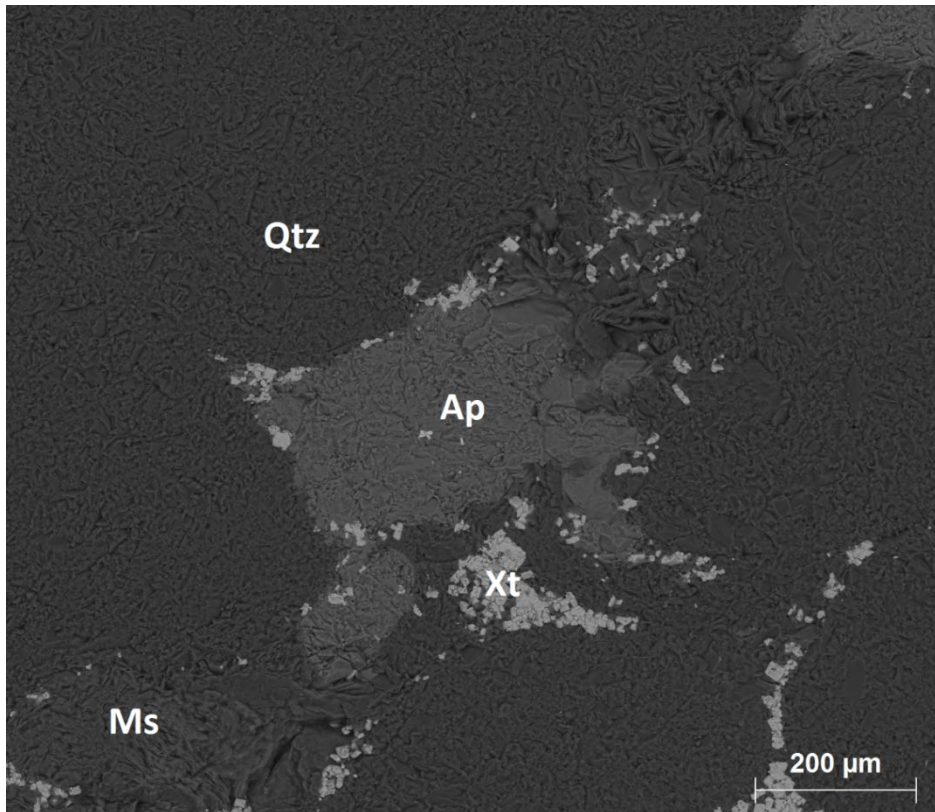


Figure 3 SEM image of quartz, muscovite, xenotime and apatite.

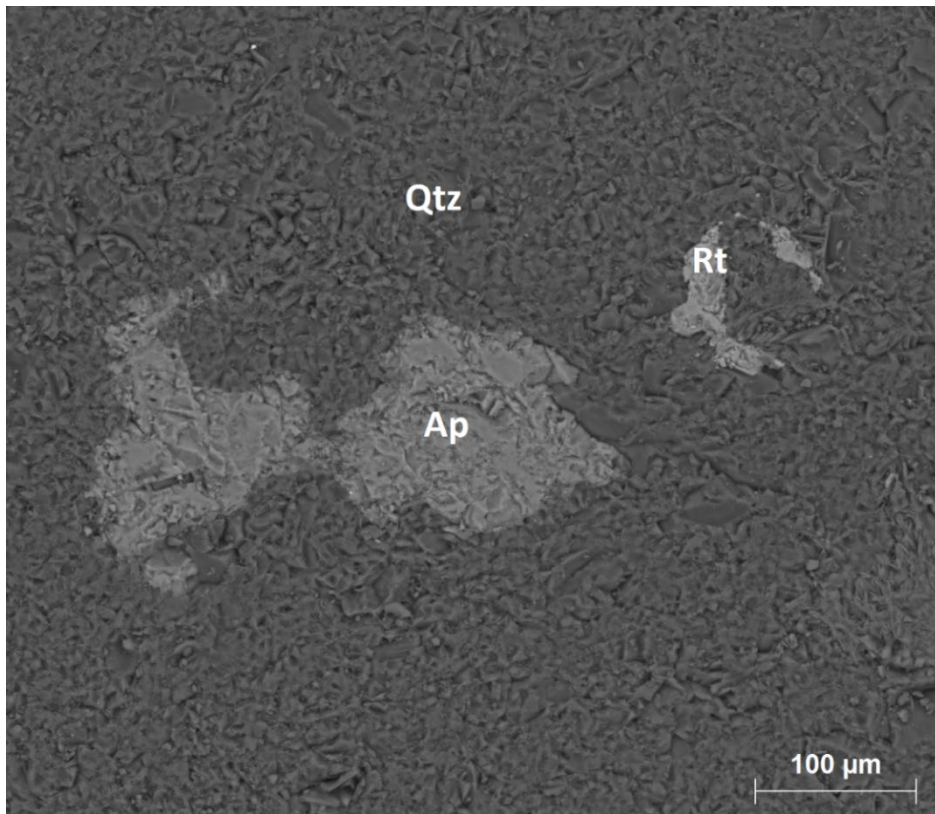


Figure 4 SEM image of apatite and rutile in quartz.

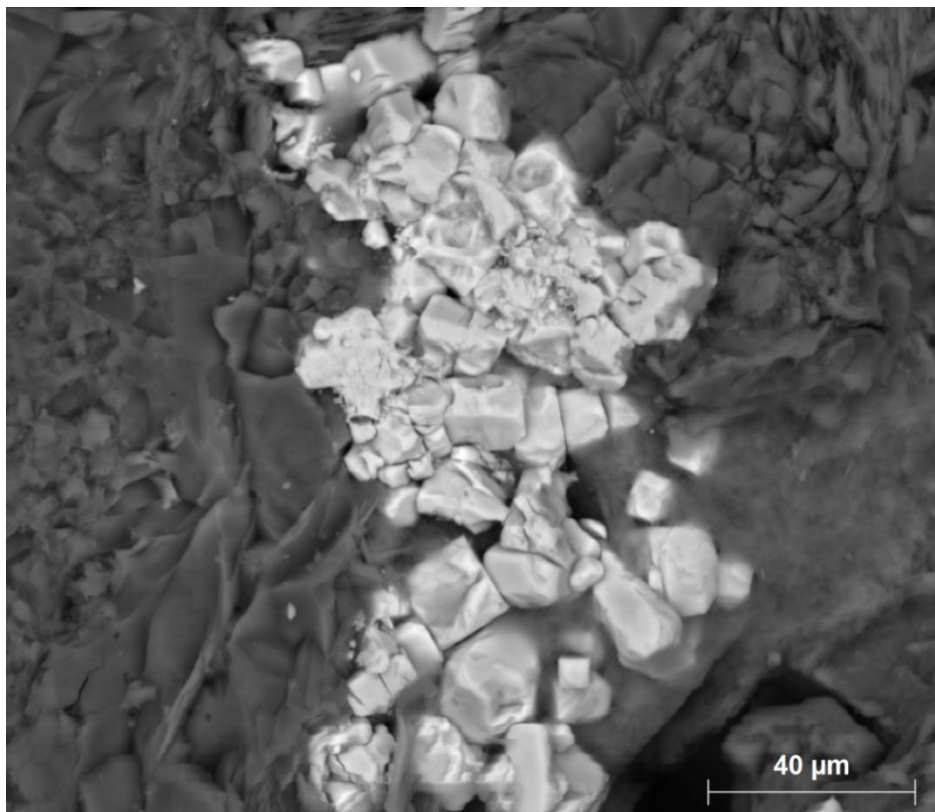


Figure 5 SEM image of xenotime in muscovite.

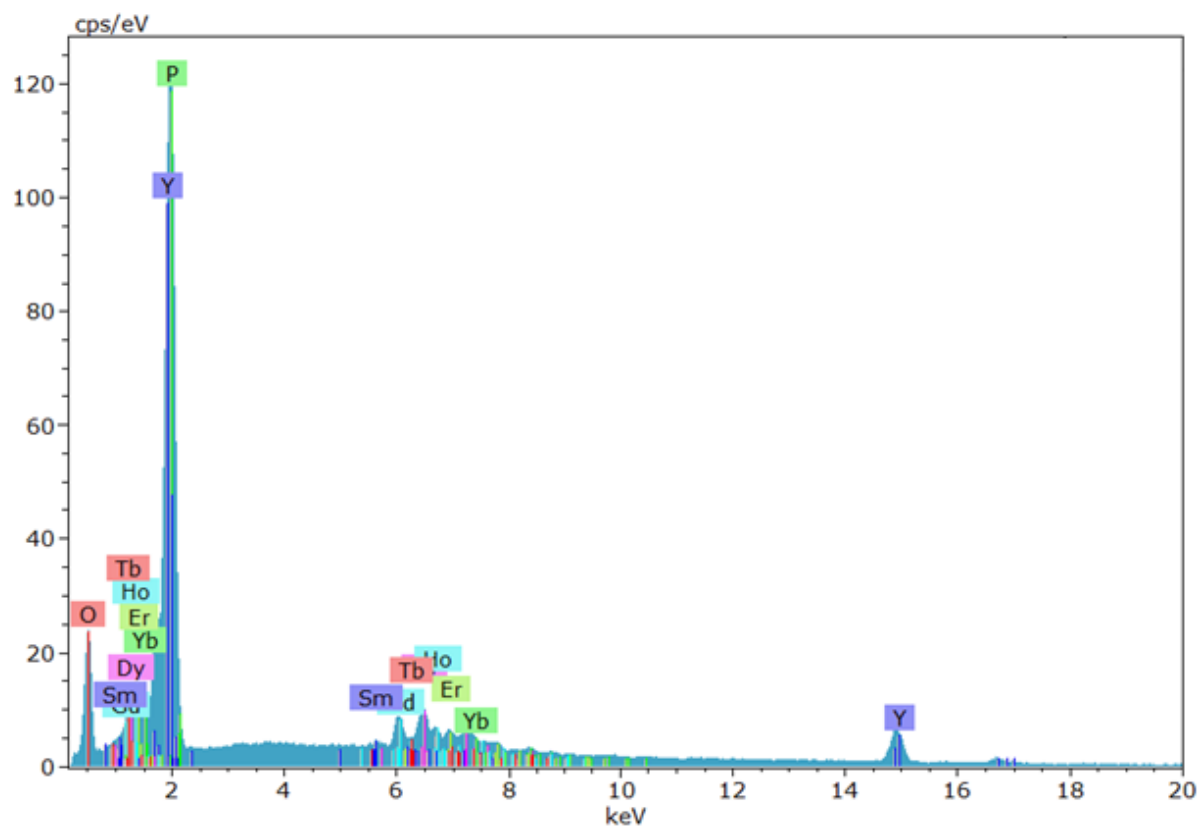


Figure 6 EDS spectra of xenotime, containing REEs Sm, Tb, Dy, Ho, Er and Yb.

	1	2	3	4	5	6	7	8
O	50.23	41.70	49.43	47.41	46.98	45.37	42.00	44.93
Na	0.00	0.00	0.00	0.00	0.00	0.00	0.00	0.51
Mg	0.59	0.66	0.70	1.18	0.75	0.81	0.51	1.08
Al	16.16	15.53	17.48	17.34	16.74	17.25	15.32	15.87
Si	29.87	22.49	27.80	25.93	26.10	24.37	23.23	24.54
K	5.75	7.37	7.72	6.45	6.93	7.12	6.87	6.04
Fe	0.00	0.89	0.58	0.58	0.90	0.53	0.50	0.60
Total	102.60	88.64	103.73	98.89	98.41	95.45	88.42	93.56

Figure 7 EDS analysis of mica crystals.

XRD

Semi-quantitative XRD analysis (Figure 8) of the sample estimates its composition to be 89% quartz, 9% muscovite, 1% xenotime and <1% rutile.

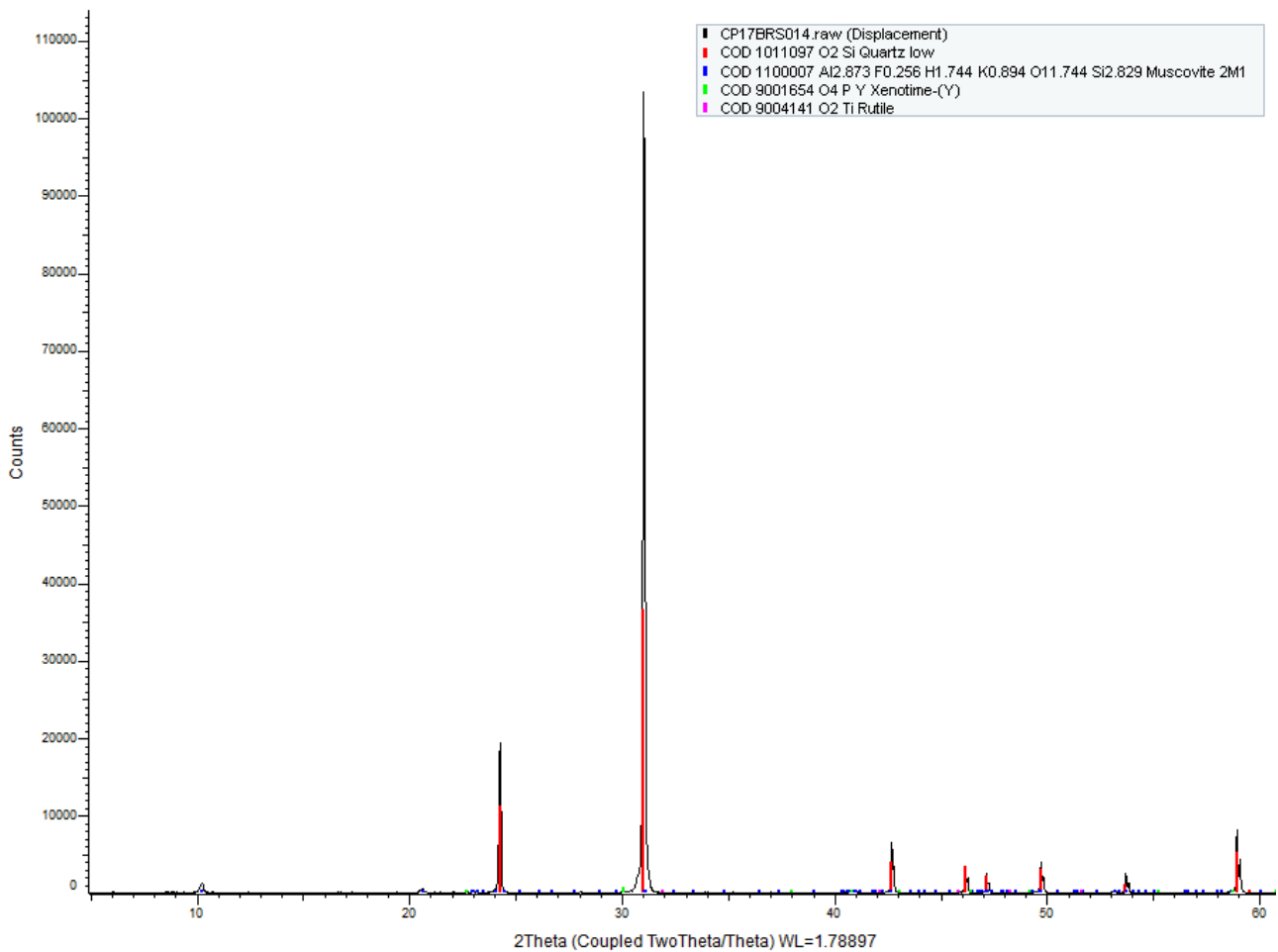


Figure 8 XRD pattern of CP17BRS014.

Full width at half maximum (FWHM) of the ca. $10.3^{\circ}2\theta$ peak tends to be lower than $0.25^{\circ}2\theta$ for micas and higher for illite (Lanson and Champion, 1991; Meunier and Velde, 2004). The measured FWHM in CP17BRS014 was 0.172, indicating that it is muscovite.

Conclusions

The geochemical results obtained with XRF and SEM identify the REE-bearing mineral xenotime in sample CP17BRS014. Based on a comparison of the VNIR-SWIR spectra with xenotime spectra published by Turner et al. (2016), the absorption features observed in Figure 1 are assigned to (features in italics are related to white mica, others due to respective REE in xenotime):

- 803 – Dy>Er, Nd?
- 933 – Dy, Yb
- 1112 – Dy
- 1276 – Dy
- 1301 – Dy
- *1400 – 2 ν OH*
- 1528 – Er>Sm
- *1910 – $\nu+\delta$ H-O-H*
- 2200, 2340, 2430 - *$\nu+\delta$ M-O-H*

Acknowledgements

This work was supported by AuScope Pty Ltd and the National Virtual Core Library (NVCL) project and CSIRO's Mineral Resources Business Unit.

References

- Lanson, B. and Champion, D. (1991) The I/S-to-illite reaction in the late stage diagenesis. *American Journal of Science*, **291**, 473-506.
- Meunier, A. and Velde, B. (2004) Illite - Origins, Evolution and Metamorphism. Springer, New York.
- Turner, D.J., Rivard, B., Groat, L.A. (2016) Visible and short-wave infrared reflectance spectroscopy of REE phosphate minerals. *American Mineralogist*, **101**, 2264-2278.